

Poster Presentations

P-28 Takashi Nagata photopigment	"A novel type of opsin with optogenetic potential: Animal opsin-based as a potential dark-active and light-inactivated G protein-coupled receptor"
P-29 Bokoku Shen	"Comparative analyses of light responses between the pineal photoreceptors expressing "bistable" and "bleaching" opsins using transgenic zebrafish"
P-30 Masaki Mizutani	"Gliding ghost of <i>Mycoplasma gallisepticum</i> "
P-31 Toshiaki Arata	"Structural dynamics of epi-genome related heterochromatin protein HP1 studied by spin labeling ESR spectroscopy"
P-32 Daiki Matsuike	"Two different conformations of Gli123 protein, essential for <i>Mycoplasma mobile</i> gliding"
P-33 Takuma Toyonaga	"Structure of motor evolved by combination of ATP synthase and phosphoglycerate kinase for <i>Mycoplasma mobile</i> gliding"
P-34 Yuya Sasajima	"Internal Ribbon Structure Driving Helicity-Switching Swimming in <i>Spiroplasma</i> "
P-35 Daichi Takahashi	"Dynamics and Structure of MreB proteins from <i>Spiroplasma eriocheiris</i> "
P-36 Hana Kiyama	"Reproduction of <i>Spiroplasma</i> swimming motility using synthetic bacteria and elucidation of its mechanism"
P-37 Maya Nakatani	"Structural and functional analysis of fatty acid kinase of <i>T. thermophilus</i> HB8"
P-38 Yuhei Tahara	"Application to microbial surface structure observation of Quick-Freeze and Deep-Etch (QFDE) replica microscopy"
P-39 Nanako Iwamoto	"The effect of Ca ²⁺ on molecular mass and viscosity of poly-γ-glutamic acid infermentative production"
P-40 Masahiro Oyama	"Exploration of novel factors related to gene expression of drug efflux pumps in <i>S. cerevisiae</i> "
P-41 Karina Yoshikawa	"Molecular dissection of the transport of the spore surface protein Isp3 in fission yeast"
P-42 Daiki Masuda	"Identification and characterization of genes involved in constructing spike structure of fission yeast spore surface"
P-43 Soichiro Seki	"Excess accumulation of carotenoids in a siphonous green alga, <i>Codium fragile</i> upon different light strengths"
P-44 Shinji Kanda	"Fabrication of Diamond/Cu Direct Bonding for Power Device Applications"
P-45 Shotaro Horikawa	"Bonding strength evaluation of Al foil/AlN junctions by surface activated bonding"
P-46 Zexin Wan	"Analysis of SiC/Si Bonding Interface with Thermal Annealing Treatment by XPS"
P-47 Takuya Higashiguchi	"Photoinduced Shape Change of Crystals Composed of a Diarylethene with a Long Alkyl Chain"
P-48 Yuya Seto	"Photoluminescence Switching of Quantum Dot Coated with Diarylethenes by Photochromic Reaction"
P-49 Katsuya Shimizu	"Bright and Tunable Emission of BODIPY in Solid State"
P-50 Kazuya Tamejima	"Simultaneous observation of nanoparticles and hexane droplets in hexane/water emulsion by quick freeze replica electron microscopy"
P-51 Daisuke Furukawa	"Study on Micro-Tomographically Functional Imaging of Blood Flow in Vascular Plexuses using Optical Coherence Doppler Velocigraphy"
P-52 Koji Yamane	"Development of Micro-tomographic Visualizing System of Mechanical Properties inside Regenerated Tissue using UA-OCDV"
P-53 Miki Yanagisawa	"Construction on Medical Diagnosing System by Photo-thermal Doppler OCT (PT-OCDV) using photosensitizer"



A Nobel Type of Opsin with Optogenetic Potential: Animal Opsin-Based Photopigment as a Potential Dark-Active and Light-Inactivated G Protein-Coupled Receptor

Takashi Nagata^{1,*}, Mitsumasa Koyanagi^{1,2}, Robert Lucas³, Akihisa Terakita^{1,2}

¹*Department of Biology and Geosciences, Graduate School of Science, Osaka City University, Osaka, Japan;* ²*OCARINA, Osaka City University, Osaka, Japan;* ³*Faculty of Biology, Medicine and Health, The University of Manchester, Manchester, UK;* *Current affiliation: *PRESTO, JST*

Peropsin or retinal pigment epithelium-derived rhodopsin homolog, found in many animals, belongs to the opsin family. Most opsins bind to 11-*cis*-retinal as a chromophore and act as light-activated G protein-coupled receptors (GPCRs). In contrast, we previously reported that peropsins from an amphioxus and a spider bind all-*trans*-retinal and isomerize it into 11-*cis* form by light [1, 2]. Such a photo-isomerization activity is also found in a retinal photoisomerase retinochrome, which serves to produce 11-*cis*-retinal chromophore in squid retinas. However, our comparative analyses of catalytic enzyme activity of peropsin and retinochrome as a retinal photoisomerase revealed that the catalytic efficiency of spider peropsin is much lower than that of squid retinochrome, suggesting a possibility of a peropsin function other than a retinal photoisomerase [3]. On the other hand, peropsin has amino acid sequence motifs that are highly conserved among GPCRs. In this study, we therefore asked whether peropsin acts as a GPCR. We conducted cultured cell-based assays for G protein activation but did not detect any significant activation of major G proteins by peropsins. Interestingly, however, chimeric mutants of peropsins constructed by replacing the third intracellular loop region with that of Gs- or Gi-coupled opsin were active and drove Gs- or Gi-mediated signaling in the dark, respectively, and were inactivated upon illumination in cultured cells. These results suggest that peropsin could act as a dark-active, light-inactivated G protein-coupled receptor. In addition, the chimeric peropsin mutants would be useful as novel optogenetic tools that enable light-inactivated G protein signaling.

- [1] Koyanagi, M.; Terakita, A.; Kubokawa, K.; Shichida, Y., Amphioxus homologs of Go-coupled rhodopsin and peropsin having 11-*cis*- and all-*trans*-retinals as their chromophores. *FEBS Lett* **2002**, 531 (3), 525-8
- [2] Nagata, T.; Koyanagi, M.; Tsukamoto, H.; Terakita, A., Identification and characterization of a protostome homologue of peropsin from a jumping spider. *J Comp Physiol A* **2010**, 196 (1), 51-9.
- [3] Nagata, T.; Koyanagi, M.; Lucas, R.; Terakita, A., An all-*trans*-retinal-binding opsin peropsin as a potential dark-active and light-inactivated G protein-coupled receptor. *Sci Rep* **2018**, 8 (1), 3535



Comparative analyses of light responses between the pineal photoreceptors expressing “bistable” and “bleaching” opsins using transgenic zebrafish.

Baoguo Shen¹, Seiji Wada¹, Emi Kawano-Yamashita¹, Mitsumasa Koyanagi^{1,2}, Akihisa Terakita^{1,2}

¹*Department of Biology and Geosciences, Graduate School of Science, Osaka City University, Osaka, Japan;* ²*OCARINA, Osaka City University, Osaka, Japan*

Pineal and related organs in lower vertebrates discriminate UV and visible light, independently of ocular color vision. We previously found that in the pineal wavelength discrimination, a pineal-specific opsin, parapinopsin serves as a UV-sensitive pigment [1-4] and has a unique molecular property called “bistable nature” different from that of visual cone opsins: upon UV-light absorption, parapinopsin converts to a stable photoproduct, which reverts to the dark state upon subsequent visible light absorption whereas the visual opsin photoproducts are unstable, release chromophores and become colorless, showing the molecular property called “bleaching” nature [1]. Therefore, it is of interest to investigate how the different photoproduct stabilities relate to photoresponses or sensitivities of photoreceptor cells. In order to obtain a clue to this issue, we established a mutant zebrafish, which expresses UV-cone opsin instead of parapinopsin in the pineal photoreceptor cells. We performed calcium imaging of photoreceptor cells of the mutant and wild-type zebrafish with a multiphoton microscope. Based on the obtained results, we discussed how the different opsin properties are involved in a light adaptation process of the pineal photoreceptor cells.

[1] Koyanagi, M.; Kawano, E.; Kinugawa, Y.; Oishi, T.; Shichida, Y.; Tamotsu, S.; Terakita, A. *PNAS* **2004**, 101, 6687-6691.

[2] Wada, S.; Kawano-Yamashita, E.; Koyanagi, M.; Terakita, A. *PLoS One* **2012**, e39003.

[3] Koyanagi, M.; Wada, S.; Kawano-Yamashita, E.; Hara, Y.; Kuraku, S.; Kosaka, S.; Terakita, A. *BMC biology* **2015**, 13, 73.

[4] Wada, S.; Shen, B.; Kawano-Yamashita, E.; Nagata, T.; Hibi, M.; Tamotsu, S.; Koyanagi, M.; Terakita, A. *PNAS* **2018**, 115, 11310-11315.



Gliding ghost of *Mycoplasma gallisepticum*

Masaki MIZUTANI¹, Makoto MIYATA^{1,2}

¹Graduate School of Science, Osaka City University, Osaka, Japan

²OCARINA, Osaka City University, Osaka, Japan

Cytadherence and/or motility are essential factors to exert pathogenicity in many infectious bacteria. Mycoplasmas are commensal and occasionally pathogenic bacteria which lack a peptidoglycan layer and have small cell and genome sizes^[1]. *Mycoplasma gallisepticum* is an avian pathogenic bacterium causing a chronic respiratory disease in chickens and an infectious sinusitis in turkeys. The infected cells transmit to their eggs from breeder birds. *Mycoplasma gallisepticum* is a related species of human pathogenic mycoplasma, *Mycoplasma pneumoniae*. They bind to sialylated oligosaccharides on host tissue surfaces and glide to spread by using unique gliding system, which is completely unrelated to other bacterial motility systems including *Mycoplasma mobile* gliding system or eukaryotic motility^[2].

A previous study has shown that the gliding motility of *Mycoplasma mobile* is driven by ATP hydrolysis on the basis of gliding ghost experiments. In this experiment, *Mycoplasma mobile* cells were permeabilized with Triton X-100 and stopped for gliding, then gliding was reactivated by the addition of ATP^[3]. However, the reactivation of permeabilized cells of *Mycoplasma pneumoniae*-type gliding has not been succeeded so far^[1].

In the present study, we permeabilized *Mycoplasma gallisepticum* cells with Triton X-100, Triton X-100 containing ADP or Triton X-100 containing ATP, and observed the behaviours of permeabilized cells. The cells permeabilized with Triton X-100 or Triton X-100 containing ADP did not show gliding. The cells permeabilized with Triton X-100 containing ATP showed gliding at a speed of $0.014 \pm 0.007 \mu\text{m/s}$ that is only 4% of intact cells, and 63% of permeabilized cells continuously glided through 17 min. Next, we permeabilized cells with Triton X-100 containing ATP and vanadate ion which gradually inhibits ATP hydrolysis. The cells permeabilized with Triton X-100 containing ATP and vanadate ion showed gliding at a speed of $0.011 \pm 0.010 \mu\text{m/s}$, and 33% of permeabilized cells continuously glided through 17 min. These results indicate that *Mycoplasma gallisepticum* gliding is also driven by ATP hydrolysis.

References

- [1] Miyata, M.; Hamaguchi, T. *Current Opinion in Microbiology* **2016**, 29, 15–21.
- [2] Nakane, D.; Miyata, M. *Journal of Bacteriology* **2009**, 191, 3256–3264.
- [3] Uenoyama, A.; Miyata, M. *PNAS* **2005**, 102, 12754–12758.



Structural dynamics of epi-genome related heterochromatin protein HP1 studied by spin labeling ESR spectroscopy

Toshiaki Arata^{1,3,4}, Shigeaki Nakazawa², Yuichi Mishima⁴, Kazunobu Sato²,
Takeji Takui², Toru Kawakami⁴, Hironobu Hojo⁴, Toshimichi Fujiwara⁴,
Makoto Miyata^{1,3}, and Isao Suetake^{4,5}

¹*Dept. Biol. and* ²*Dept. Chem., Grad. Sch. Sci., and* ³*OCARINA, Osaka City Univ., Osaka;*
⁴*Inst. Protein Res., Osaka Univ., Osaka;* ⁵*Koshien Univ., Hyogo, Japan*

Heterochromatin protein (HP1) is evolutionally conserved, and binds to epigenetic mark, lysine9 methylated histone H3 as a transcriptional repressor [1]. Here, we introduced site-specific spin labeling on HP1 and examined the dynamics of human HP1 with continuous wave (CW)-ESR and pulsed electron double resonance (DEER/PELDOR) spectroscopy [2,3]. HP1 has the chromodomain (CD) and the chromoshadow domain (CSD), which are linked by the flexible HR. It dimerizes *via* CSD to form NTE-CD-HR-CSD-CSD-HR-CD-NTE, where NTE is an N-terminal extension of CD. The ESR spectroscopy from the nitroxide spin label fixed at a cysteine of the CD or CSD of human HP1 indicated a highly flexible structure of HP1 molecule on nanosecond time scale. Different from yeast HP1, dimerization *via* CD-CD interaction is reported, CD was freely mobile by CW-ESR and the distance between two CD domains in the HP1 dimer was beyond the limit of DEER (>7 nm). HP1 is reported to bind lysine9 methylated histone H3 peptide (H3K9me) at CD domain and also bind DNA at HR domain while HP1 γ does not bind DNA. The rotational dynamics of CD slowed down 1.5-fold by H3K9me either as CD alone or in full-length HP1, and also indirectly by DNA while that in HP1 γ did not. Preliminary results showed that phosphomimic mutation of NTE slowed down CD dynamics 1.5-fold in full-length HP1 but made it apparently insensitive to DNA and H3K9me binding. The NTE region will play an important role for HP1 function by controlling the CD dynamics in phosphorylation-dependent manner. The HR which links between CD and CSD was highly dynamic on subnanosecond time scale as detected by CW-ESR. Dynamics of spin label located at several residues of HR in HP1 α was restricted weakly with DNA only under high viscosity in glycerol. This weak motional restriction suggested loose translational diffusion of HP1 α on DNA and *vice versa*. In contrast, the other domain (CSD) stably formed a dimer, while the interdomain distance was just expected based on crystal structure. In addition, the CSD dimer in full-length HP1 exhibited nearly free but isoform-specific motion; HP1 α was 1.5-fold slower than HP1 γ , but became identical when the N-terminal domain including HR was deleted. The distinct dynamics is due to the fact that HR is different between HP1 α and HP1 γ in length and sequence. It is likely that distinct dynamics contributes to the isoform-specific function of HP1.

[1]Mishima,Y.*et al.Nuc.Acid Res.***2015**,43,10200.[2]Abe,J.*et al.Appl.Mag.Reson.***2018**,42,473.
[3]Arata,T. (In Japanese) *Seibutsu Butsuri* **2012**, 4, 172; *Bunko Kenkyu* **2006**, 54, 245.



Two different conformations of Gli123 protein, essential for *Mycoplasma mobile* gliding

Daiki Matsuike¹⁾, Yuhei O Tahara¹⁾, Tasuku Hamaguchi³⁾,
Hisashi Kudo⁴⁾, Yuuki Hayashi⁴⁾, Munehito Arai⁴⁾, Makoto Miyata^{1,2)}

1) Department of Biology, Graduate School of Science, Osaka City University,

2) OCARINA, Osaka City University

3)RIKEN, SPring-8 Center

4) Graduate School of Arts and Science, The University of Tokyo

Abstract: *Mycoplasma mobile*, a fish pathogenic bacterium glides on solid surfaces based on ATP energy by a unique energy-conversion mechanism. Four huge proteins clustering on the surface of gliding machinery are essential for this mechanism. Gli349 shaped like an eighth music note (♪), acts as a leg protein by binding to sialylated oligosaccharides on solid surfaces. Gli521 shaped an interrogation mark (?), transmits the force to Gli349 as a crank protein [1]. We focused on the structure of Gli123, a 123 kDa protein responsible for the assembly of surface gliding proteins [2].

Gli123 showed two different conformations under rotary-shadowing electron microscopy (EM), i.e. globular and rod structures in high and low ionic strength conditions, respectively. This conformational shift occurred reversibly as monitored by light scattering. We clarified the globular structure by single particle analysis of negative staining EM, as a "White-mushroom" with dimensions, 20.0, 14.5, and 16.0 nm. Reconstruction of higher resolution is undertaken by using cryo-EM. We clarified the rod structure by Small Angle X-ray Scattering (SAXS) analyses, as chained five masses about 34 nm long and 4 nm wide. We are currently also trying SAXS modeling of globular structure.

On the surface of gliding machinery, four proteins are organized to form a large complex. The conformational change of Gli123 may be involved in this organizing process.

Keywords

Mycoplasma mobile / Electron Microscopy / single particle analysis / SAXS

References:

[1] Miyata, M.; Hamaguchi, T. *Current Opinion in Microbiology* **2016**, 29, 15-21.

[2] Uenoyama, A.; Miyata M. *Journal of Bacteriology* **2005**, 187, 5578-5584.



Structure of motor evolved by combination of ATP synthase and phosphoglycerate kinase for *Mycoplasma mobile* gliding

Takuma Toyonaga¹, Takayuki Kato², Akihiro Kawamoto³, Tasuku Hamaguchi⁴
Noriyuki Kodera⁵, Toshio Ando⁵, Keiichi Namba^{2,4,6} and Makoto Miyata^{1,7}

¹Grad. Sch. Sci., Osaka City Univ., Japan, ²Grad. Sch. Front. Biosci., Osaka Univ., Japan,
³IPR, Osaka Univ., Japan, ⁴SPRING-8, Riken, Japan,
⁵WPI NanoLSI, Kanazawa Univ., Japan, ⁶BDR, Riken, Japan
⁷OCARINA, Osaka City Univ., Japan

Mycoplasma mobile, a fish pathogenic bacterium, glides on host cell surfaces with a unique mechanism. The gliding machinery is divided into two parts: internal and surface structures. Our previous study showed that the motor in the internal structure including an ATP synthase homolog and phosphoglycerate kinase (PGK) forms chains along the cell membrane [1, 2]. Both ATP synthase and PGK are essential enzymes for life in most living organisms and synthesize ATP in electron transport chain and glycolytic pathway, respectively. Recently, electron cryomicroscopy (cryoEM), which can visualize biomolecules in a frozen hydrated state has been developed drastically, resulting in resolving biomolecular structures at near atomic resolution. In the present study, we determined the structure of the internal motor by single-particle cryoEM at 7.4 Å resolution. The structure showed that two hexamers are paired by a rectangular frame with eight arm-like extensions. This structure allowed us to dock the crystal structure of ATP synthase catalytic subunits from *Bacillus sp.* into the two hexamers at secondary-structure level. PGK was assigned to each of four arms extending horizontally from the homolog of ATP synthase catalytic subunits. A coiled-coil structure deeply penetrates the center of hexamers, as seen in ATP synthases generally. The coiled coil should be composed of MMOB1630, which has no homology with any subunit of ATP synthase, based on analyses of isolated single hexamer including the coiled coil. Our data suggested that the motor of *Mycoplasma mobile* evolved by the combination of two essential enzymes for life with several novel proteins.



Figure. CryoEM structure of the internal motor fitted with atomic models of ATP synthase from *Bacillus sp.* (α -subunits, red; β -subunits, yellow; PDB ID code 2QE7 [3]) and PGK from *Thermus sp.* (blue; PDB ID code 2IE8 [4]).

- [1] Miyata, M.; Hamaguchi, T. *Curr. Opin. Microbiol.* **2016**, 29, 15-21.
[2] Nakane, D.; Miyata, M. *Proc. Natl. Acad. Sci. USA* **2007**, 104, 19518-19523.
[3] Stocker, A.; Keis, S.; Vonck, J.; Cook, G.M.; Dimroth, P. *Structure* **2007**, 15, 904-914
[4] Lee, J.H.; Im, Y.J.; Bae, J.; Kim, D.; Kim, M.K.; Kang, G.B.; Lee, D.S.; Eom, S.H. *Biochem. Biophys. Res. Commun.* **2006**, 350, 1044-1049



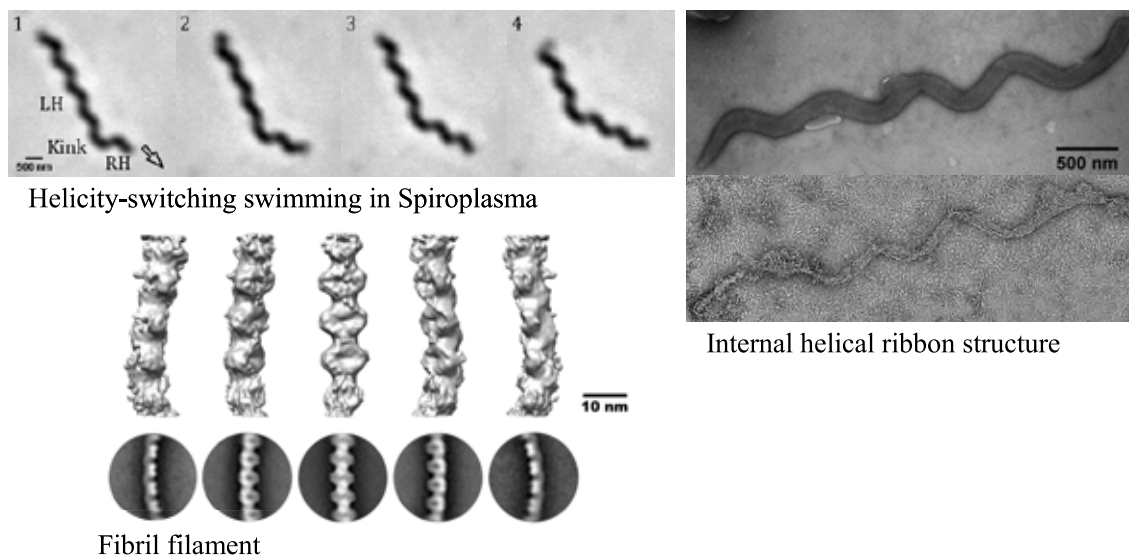
Internal Ribbon Structure Driving Helicity-Switching Swimming in Spiroplasma

Yuya SASAJIMA¹⁾, Makoto MIYATA^{1,2)}

¹⁾ Graduate School of Science, Osaka City University, Japan

²⁾ OCARINA, Osaka City University, Japan

Spiroplasma eriocheiris, a helical-shaped swimming bacterium lacking peptidoglycan layer, a bacterial cell wall, swims in a high viscosity solution by reversing its helical orientation from front to back [1, 2, 3]. In the present study, we analyzed the ribbon of about 110 nm in width that exists inside the helical helix by electron microscopy, to elucidate the mechanism of helical reversal. The isolated ribbon had 840 nm pitch very similar with the cell. The protofilament obtained by separating the ribbon was a double helix composed of fibers in a ring-like repeating structure, the pitch of which was roughly consistent with the pitch of the ribbon and the cell. Based on these observations, we concluded that the swimming is caused by the structural change in Fibril protein forming protofilaments of about 11 nm in diameter. When the ribbon containing three kinds of MreB protein in addition to Fibril was treated with A22, MreB polymerization inhibitor, separation of each bundled protofilament was observed, suggesting that the MreBs orient fibril filaments to the ribbon. Therefore, any of these four proteins is expected to be responsible for the helical switch. We are clarifying the structure and its changes of isolated Fibril by using electron microscopy and single particle analysis.



[1] Miyata M and Hamaguchi T. *Frontiers in Microbiology*. 2016, 7, 960.

[2] Terahara N, Tulum I, and Miyata M. *Biochemical and Biophysical Research Communication*. 2017, 487, 488-93.

[3] Liu P, Zheng H, Meng Q, Terahara N, Gu W, Wang S, Zhao G, Nakane D, Wang W, and Miyata M. *Frontiers in Microbiology*. 2017, 8, 58.



Dynamics and Structure of MreB proteins from *Spiroplasma eriocheiris*

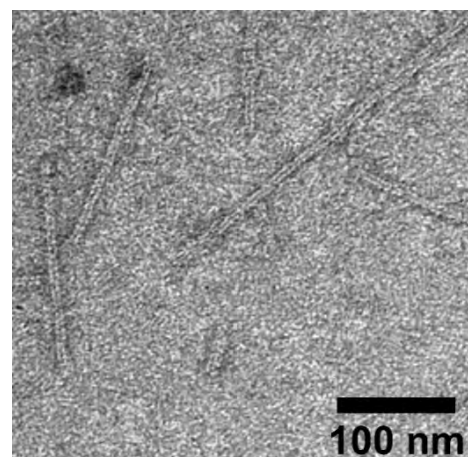
Daichi Takahashi¹, Makoto Miyata^{1,2}

1. Graduate School of Science, Osaka City University
2. OCARINA, Osaka City University

Abstract: MreB is a bacterial protein capable of polymerization using ATP (adenosine 5'-triphosphate) and Mg^{2+} [1]. The polymer of MreB play a critical role to form rod shapes of bacteria by binding to the inside of the cell membrane [2]. MreB is coded as a single copy of gene in many bacteria, and its role has been considered to be conserved. A novel type MreBs were discovered in genus *Spiroplasma* belonging to the same class with *Mycoplasma* [3]. Each *Spiroplasma* species has more than five classes of MreBs. These MreBs are thought to be involved in making *Spiroplasma* helical shapes and twisting their bodies for swimming motility [4]. To clarify the characters of these novel MreBs, two kinds of MreBs (MreB3 and MreB5) among five derived from *Spiroplasma eriocheiris* were purified and analyzed for the structures and the polymerization dynamics. When these MreBs were put into a polymerization condition, paired two filaments were observed under electron microscopy. The structure was similar to MreBs of other species. Both MreB3 and 5 required 1.5 to 2 hours for the equilibration of polymerization although conventional MreBs needed only 20 - 30 minutes as traced by light scattering technique. Polymerizations by using GTP (guanosine 5'-triphosphate) were faster than by using ATP. Addition of Mg^{2+} slowed the polymerization of these MreBs, although increase of Mg^{2+} made polymerization of conventional MreBs faster. Sedimentation experiments suggested that more than half of the MreBs remained as monomers although more than half polymerized in conventional MreBs [1]. These results suggest that MreBs from *Spiroplasma eriocheiris* have evolved a unique reaction mechanism and lower polymerization ability.

References

- [1] Bean GJ *et al. Biochemistry* **2008**, 47, 826-35.
- [2] Salje J *et al. Mol Cell* **2011**, 43, 478-87.
- [3] Ku C *et al. Biochem Biophys Res Commun* **2014**, 446, 927-32.
- [4] Liu P *et al. Front Microbiol* **2017**, 8, 58.





Reproduction of *Spiroplasma* swimming motility using synthetic bacteria and elucidation of its mechanism

Hana Kiyama¹, Shigeyuki Kakizawa², and Makoto Miyata^{1,3}

1. Graduate School of Science, Osaka City University, Japan

2. The National Institute of Advanced Industrial Science and Technology (AIST)

3. OCARINA, Osaka City University, Japan

The class *Mollicutes*, a small group of bacteria, is thought to have caused extraordinary evolution. *Spiroplasma*, belonging to class *Mollicutes*, performs a unique swimming motility by switching the helical core of cell clockwise and counterclockwise. The cell helicity is composed of Fibril protein unique to *Spiroplasma* genus and five classes of MreB homologous to eukaryotic actin [1]. MreB is a universal protein in bacteria and acts as a scaffold for cell wall synthesis by forming short filaments [2], but interestingly it is involved in swimming motility in *Spiroplasma* which does not have a cell wall. In this study, for the purpose of reproducing swimming motility, a group of genes involved in *Spiroplasma eriocheiris* swimming was introduced and expressed in synthetic bacteria (*Mycoplasma mycoides* JCVI-syn3.0B) having no motility at all [3]. Synthetic bacteria made from mycoplasma have a genome designed only with essential genes.

When Fibril protein was expressed, about 30% cells elongated 4.4 times longer than the original. In addition, about 26% of the elongated cells formed a clear helicity with a pitch of 0.66 μm , similar to that *S. eriocheiris* shows in the starved state. The filaments isolated from these synthetic bacteria and observed by electron microscopy were very similar to the Fibril filaments from *S. eriocheiris*.

In addition, when MreB2, the most abundant MreB in *S. eriocheiris* was expressed, about 11% of the cells expanded to filamentous form with a length of 3.0 times. When MreB2 fused with mCherry was expressed, intense fluorescence was observed in the filamentous part.

As the cell shape can be changed by expressing genes in synthetic bacteria, the *Spiroplasma* swimming motility can be reproduced by further expressing the genes involved in swimming in the future studies.

[1] Liu, P. *et al. Front Microbiol.* **2017**, 8, 58.

[2] Shi, H. *et al. cell.* **2018**, 172, 1294-1305.

[3] Hutchison, CA 3rd. *et al. Science.* **2016**, 351, aad6253.





Structural and functional analysis of fatty acid kinase of *Thermus thermophilus* HB8

Maya Nakatani¹, Taihei Murakami^{1,2}, Hiroki Okanishi^{3,4}, Norie Araki⁴,
Makoto Miyata^{1,5} and Ryoji Masui¹

¹Grad. Sch. Sci., Osaka City Univ., ²Fac. Sci. Eng., Waseda Univ., ³Grad.
Sch. Med., Osaka Univ., ⁴Grad. Sch. Med. Sci., Kumamoto Univ.,
⁵OCARINA, Osaka City Univ.

Fatty acid kinase (Fak), which has been identified recently [1], consists of two subunits, FakA and FakB. FakA phosphorylates the fatty acid bound to FakB. Fak is essential for synthesis of membrane lipids in bacteria such as *Mycoplasma* that do not have fatty acid synthase. Furthermore, Fak is reported to be involved in gene expressions of virulence factors. However, the structure and reaction mechanism of Fak remain largely unknown. In this study, we analyzed the subunit composition and domain organization of Fak from *Thermus thermophilus* HB8 (ttFak). Fatty acid kinase subunit of ttFak, TTHA0214 (ttFakA), was overexpressed in *E. coli* and purified to homogeneity. ttFakA was shown to be monomeric, which differs from the result of the previous study [1]. Pull-down assay using the cell extract of *T. thermophilus* coupled with mass spectrometry revealed that ttFakA interacts with TTHA0951 (ttFakB1), which is a fatty acid binding protein belonging to DegV family. Native PAGE also detected interaction of ttFakA with another DegV family protein TTHA0950 (ttFakB2). These results suggested that these three proteins, ttFakA, ttFakB1, and ttFakB2 constitute ttFak. Limited proteolysis of ttFakA with two proteases yielded two fragments of almost the same sizes each of which corresponded to the N- and C-terminal fragments. This agreed to the sequence-based prediction that ttFakA consists of two domains. The observation that the resulted fragments could not be separated by gel filtration suggested that the N- and C-terminal domains strongly interact with each other. Unexpectedly, when ttFakA was incubated with ATP in the presence of divalent cations, ttFakA was auto-phosphorylated. By mass spectrometry, the major phosphorylation site was identified as Ser249, which was reported to be phosphorylated in the previous proteomic analysis [2]. In the predicted structure, N-terminal domain might be the catalytic domain containing the ATP-binding site and Ser249 might be located in the loop region between the two domains. Based on these results, we discuss the structural organization and the role of auto-phosphorylation of ttFakA.

[1] Parsons, J. B., Broussard, T. C., Bose, J. L., Rosch, J. W., Jackson, P., Subramanian, C. and Rock, C. O. *Proc. Natl. Acad. Sci. U. S. A.* **2014**, 111, 10532-10537.

[2] Wu, W., Liao, J., Lin, G., Lin, M., Chang, Y., Liang, S., Yang, F., Khoo, K. and Wu, S. *Mol. Cell. Proteomics* **2013**, 12, 2701-2713.



Application to microbial surface structure observation of Quick-Freeze and Deep-Etch (QFDE) replica microscopy

Yuhei O Tahara^{1,2}, Makoto Miyata^{1,2}

1)Graduate School of Science, Osaka City University, Japan

2)OCARINA, Osaka City University, Japan

Quick-Freeze and Deep-Etch (QFDE) replica microscopy is an electron microscopy method in which a sample is frozen and fixed in a moment by hitting a sample against a cooled metal and metal coated to exposed sample surface, and observed the metal membrane with resolution of nanometer order and time resolution of submillisecond.

In this technology, it is possible to observe the microstructure on the sample surface with high contrast, and it is particularly suitable for the surface of microorganisms.

This technology was developed and implemented in the new academic field, Ministry of Education, Culture, Sports, Science and Technology in 2012 - 2016. As technical support from 2018, 24 researchers and students from 16 research groups inside and outside the campus conducted a rapid freeze replica method and related electron microscope observations for 180 days in total.

- 1, *E. coli* infected with T phage (Fig. 1)
- 2, S-layer structure of *Caulobacter crescentus*
- 3, Intracellular structure of vesicle-releasing bacteria (Fig.2)
- 4, Detailed structure of artificial synthesis life Syn 3.0 (Fig. 3)
- 5, Surface structural change during germination of fission yeast spores (Fig 4)



Fig.1



Fig. 2



Fig.3



Fig.4

The effect of Ca^{2+} on molecular mass and viscosity of
poly- γ -glutamic acid fermentative production



Presenter Nanako IWAMOTO¹, Yoshihiro YAMOGUCHI^{1,2},
Akira OGATA^{1,3}, Toshio TANAKA¹, Ken-ichi FUJITA¹

Affiliation ¹ *Grad. Sch. Sci. Osaka City Univ.*

² *OCARINA, Osaka City Univ.*

³ *Res. Center. Urban Health & Sports, Osaka City Univ.*

Poly- γ -glutamic acid (PGA) is one of high viscous constituents of Japanese traditional fermentative food Natto. When PGA is left at room temperature, gradual decrease in its molecular mass is observed as incubation period increasing. Decrease in the molecular mass is accelerated by heat treatment at 100°C. We previously reported that decrease in molecular mass occurred by heat treatment is restricted by divalent metal cation chelating agents such as EDTA and citric acid. In addition, the restrictive effect is enhanced by the Ca^{2+} -specific chelating agents such as BAPTA and EGTA. Based on the results, we assumed the involvement of Ca^{2+} in decrease in molecular mass of PGA occurred by heat treatment and increase in molecular mass during fermentative production of PGA. In this study, PGA was fermentatively produced using a synthetic culture medium with or without Ca^{2+} and we then estimated the molecular mass of PGA obtained.

We found that viscosity of the culture supernatant disappeared and the molecular mass of PGA was relatively low in the case using Ca^{2+} less synthetic medium. The low molecular mass is thought to depend on low L-glutamic acid concentration in the synthetic medium. Therefore, L-glutamic acid concentration was elevated to 10 fold in the medium. As a result, viscosity still disappeared in the culture supernatant. However, the molecular mass was equally high as compared with a control PGA sample. These results obtained above could not explain the involvement of Ca^{2+} in heat sensitive nature of PGA molecules. Therefore, further investigations are in progress to prove the involvement.



Exploration of novel factors related to gene expression of drug efflux pumps in *S. cerevisiae*

Masahiro Oyama¹, Yoshihiro Yamaguchi^{1,2}, Akira Ogita^{1,3},
Toshio Tanaka¹, Ken-ichi Fujita¹

¹*Graduate School of Science, Osaka City University,*

²*OCU Advanced Research Institute for Natural Science and Technology,*

³*Research Center for Urban Health and Sports, Osaka City University*

Abstract: Recently, drug-resistant fungi have been frequently emerged by abuse of antifungal drugs. Especially resistant fungi against azole drugs are the problem in clinical sites [1]. Combining drugs that restrict drug resistance mechanisms with already approved drugs is one of the superior methods for overcoming infection caused by drug-resistant fungi. We have reported that trans-anethole (anethole), which is the principal component of anise oil, inhibits the drug efflux [2]. When *S. cerevisiae* cells were treated with dodecanol, viable cell number temporally reduced. Anethole restricted over-expression of multidrug efflux pump's gene *PDR5* induced by dodecanol to control levels thereby expressing durable antifungal effects. However, the detailed mechanism has been unsolved.

At first, we examined the susceptibility of dodecanol in gene-deficient strains related to regulation of intracellular Ca^{2+} levels. Among them, *pmr1Δ* was highly susceptible to dodecanol. Next, we examined the change in cell viability of *pmr1Δ*. The recovery of the cell viability delayed in treatment with dodecanol. We indicated that the involvement of *PMR1* in over-expression of *PDR5* induced by dodecanol. Increase in intracellular Ca^{2+} levels was significantly observed in treatment with dodecanol and combination of dodecanol with anethole. Furthermore, *pmr1Δ* maintained elevated Ca^{2+} levels as compared with the parental strain. The expression of *PMR1* was restricted in the treatment with dodecanol and drug combination. Dodecanol did not induce the expression of *PDR5* in *pmr1Δ*. Above all, we suggested that elevated Ca^{2+} levels provably depend on the decreased expression level of *PMR1* caused by dodecanol. In addition, the elevated Ca^{2+} levels possibly restrict over-expression of *PDR5*.

References:

[1] Masiá Canuto M.; Gutiérrez Rodero F. *Lancet Infect. Dis.* **2002**, 2, 550.

[2] Fujita, K.; Ishikura, T.; Jono, Y.; Yamaguchi, Y.; Ogita, A.; Kubo, I.; Tanaka, T. *Biochim. Biophys. Acta Gen. Subj.* **2017**, 1861(2), 477.

Molecular dissection of the transport of the spore surface protein Isp3 in fission yeast.



Karina YOSHIKAWA¹, and Taro NAKAMURA^{1,2}

1) Graduate School of Science, Osaka City University, Japan

2) The OCU Advanced Research Institute for Natural Science and Technology (OCARINA), Osaka City University, Japan

Spores of fission yeast are dormant cells resistant to various stresses such as heat and alcohol. To date, we have found that the outermost layer of the fission yeast spore wall is composed of a protein called Isp3 (Isp3 layer) and that the Isp3 layer plays an important role in spore tolerance to environmental stresses [1]. Isp3 is a protein that is specifically found in fission yeast and has very characteristic regions (Fig. 1). Isp3 is expressed

```
MGLGNLCSYKQDDSLDILQKKVLIDAFNKVTIDC
PNVQHQQPTYWYPPPPRHHKEHKKSHHHWE
SDDSSDDEESCEKKKPKKCEKKKPKCES
EQNNGCGRRNQLARRLAFLGSFGDGDGDCGN
AFTVTGPITYFRTCPDPLTGITPAVAAAAAATPA
AATPATPAAAATPAAPAA
```

Blue: the basic amino acid-rich region.
Red: the acidic amino acid region.
Pink: the repeat sequence. Green: the alanine-rich region.

specifically during sporulation, accumulates in the forming spores and subsequently exported to the outside of the spore, i.e. the cytoplasm of the ascus. Since signal sequence is not found in Isp3, it is possible that Isp3 may be transported by an unknown mechanism. The aim of this study is to address the novel mechanism of protein transport using Isp3 as a model.

The various deletion mutants of Isp3 were constructed and their localizations were observed. Surprisingly, the characteristic regions as described above were not involved in the export. Isp3 lacking the N terminal 45 amino acids accumulated in the spores. These data suggest that the N-terminal region is necessary for export of Isp3 (Fig. 2).



Figure 2. The images show the presence of Isp3-GFP and ΔN-terminal region-GFP in sporulating cells.

[1] Fukunishi, K. et al., *Mol. Biol. Cell* **2014**, 25, 1549-1559



Identification and characterization of genes involved in constructing spike structure of fission yeast spore surface

Daiki Masuda¹, Yuhei Tahara^{1,2}, Makoto Miyata^{1,2}, and Taro Nakamura¹

² The OCU Advanced Research Institute for Natural Science and Technology (OCARINA),
Osaka City University, Japan

Introduction: Fission yeast spore surface is covered by the characteristics spike structure. How is this spike structure constructed? *mde10*⁺ was identified as a gene involved in the construction of the spike structure^[1] (Figure). *mde10*⁺ encodes an ADAM family protein which is conserved widely in higher organisms including human. ADAMs are responsible for important life phenomena on cell surface such as membrane fusion of sperm and egg or signaling, in association with various proteins. Therefore, we assumed that the additional genes cooperate with *mde10*⁺ to construct spike structure. The aim of this study is to identify and characterize the additional genes involved in constructing the spike structure and elucidate its molecule mechanism.

Results: To identify target genes, we observed 191 deletion strains of genes whose expression are upregulated during sporulation (*mug* and *meu*)^{[2][3]}. At first, we roughly selected 40 mutants whose spore periphery was different from wild-type by phase contrast microscopy. Next, we observed the fine structure of these strains by electron microscopy and identified 10 mutants, two of which (*mug57* Δ and *meu30* Δ) exhibited abnormal surface morphology. *mug57*⁺ and *meu30*⁺ encode a fasciclin I domain protein which is involved in cell adhesion and an α -amylase homolog, respectively. Interestingly, although spike structure remained in these mutants, they were smaller and a number of spike was increased. These data suggest that the presense of pathway to surpress the number of spike structure on the spore surface.

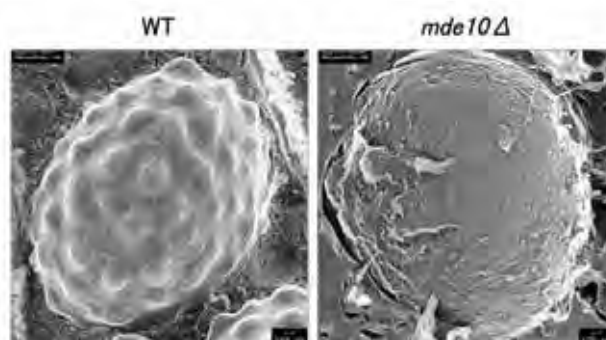


Figure. Fission yeast spore by electron microscopy

[1] Nakamura T *et al. Eukaryotic Cell* 2004, 3, 27-39.

[2] Martin C *et al. Curr Biol* 2005, 15, 2056-2062.

[3] Watanabe T *et al. Nucleic Acids Res* 2001, 29, 2327-2337.



Excess accumulation of carotenoids in a siphonous green alga, *Codium fragile* upon different light strengths

Soichiro Seki¹, Ryuichi Kano², Ritsuko Fujii^{1,2,3}

¹Department of Chemistry, Faculty of Science, ²Graduate school of Science, and ³The OCU Advanced Research Institute for Natural Science and Technology, Osaka City University, Japan

The major carotenoids accumulated in chloroplast of higher plants and algae are highly conserved: β -carotene, lutein, violaxanthin (Vx) and neoxanthin. Solo conformation of neoxanthin as 9'-*cis* has been reported for more than 140 species [1], but several "primitive" green algae were reported to contain all-*trans* neoxanthin (tNx) [2]. Our group has shown for the first time that the accumulation of tNx is associated to the strong illumination during cultivation for *Codium intricatum* [3]. *Codium* sp. belongs to the "siphonous alga" which is a branch of green algae accumulating siphonaxanthin (Sx) and/or siphonein (Sn), and α -carotene instead of lutein and β -carotene, respectively. These species show negligible "xanthophyll cycle" [4], which is a well-known photoprotective adaptation of green lineage including accumulation of Vx upon strong light exposure. Therefore, we addressed a question that accumulated tNx may be involved in an unknown photoprotective adaptation representative to the xanthophyll cycle.

In this study, we focused on to clarify the precise relationship between accumulation of tNx and photosynthetic photon flux density (photon flux density of 400 to 700 nm photons, PPFD, in $\mu\text{mol photon m}^{-2} \text{sec}^{-1}$). We cultivated the gametophyte of *C. fragile* having 50 μm i.d. filamentous form (Kobe University Macro-Algal Culture Collection, KU-0654). Approximately 0.7 g (wet weight) aliquots of the cultivated cells were put into glass vials (32 mm inner diameter) and were incubated under four different irradiation strengths of 50, 100, 200, 300 PPFD from white LED for 7 days. Pigment compositions were determined by using HPLC system [3] and normalized with eight molecules of chlorophyll *b*.

As shown in the Fig. (a), the relative number of tNx increased with the incubation days at all irradiation strengths tested. It also increases with irradiation strengths as plotted in Fig. (b). Interestingly, the increment of tNx accumulation was large for 0-100 PPFD and about one sixth for 100-300 PPFD. This may indicate that the numbers of tNx may reach a sort of saturation in thylakoid membranes between 100-200 PPFD, and the photoprotective adaptation also reaches the maximum at the irradiation condition if tNx plays photoprotective function. Further experiments are necessary to clarify this.

<References>

1. Takaichi, S.; Mimuro, M. *Plant Cell Physiol.* **1998**, *39*(9), 968–977.
2. Yoshii, Y. *Phycolog. Res.* **2006**, *54*, 220–229.
3. Urugami, C. et al. *Photosynth. Res.* **2014**, *121*, 69-77.
4. Giovagnetti, V. et al. *Planta* **2018**, *247*(6), 1293-1306.

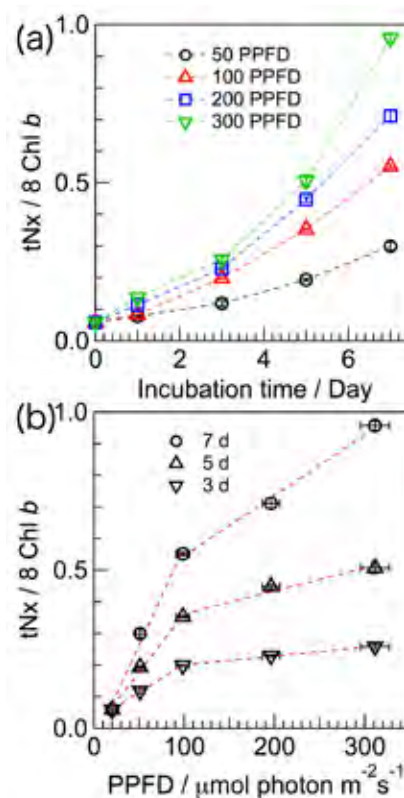


Figure. Relative numbers of all-*trans* neoxanthin (tNx) in cultivated *Codium fragile* against incubation time (a) and irradiance (b).



Fabrication of Diamond/Cu Direct Bonding for Power Device Applications

Shinji Kanda¹, Satoshi Masuya², Makoto Kasu², Naoteru Shigekawa¹, and
Jianbo Liang¹

¹*Graduate School of Engineering, Osaka City University,
3-3-138 Sugimoto, Sumiyoshi-ku, Osaka 558-8585, Japan*

²*Department of Electrical and Electronic Engineering, Saga University,
1 Honjo-machi, Saga 840-8502, Japan
m18tb019@ab.osaka-cu.ac.jp*

Abstract:

Diamond is the best potential candidate as the next generation semiconductor material for high power and high frequency devices^{[1],[2]}. Diamond devices with high frequency, high thermal stability, high-current and low-loss capability have been reported^{[3]-[5]}. The high operating electrical power in such devices would result in an increase in temperature near the active region, which would degrade devices performance and reliability.

Power devices were generally directly mounted onto the heat sink by solder bonding or hydrophilic bonding. However, the thermal conductivity of the solder materials is very low in comparison with those of metals such as Cu and Al. The thermal resistance of the solder layer limits the heat dissipation of the devices. We previously reported the direct bonding of diamond and Al using surface activated bonding (SAB) at room temperature and obtained diamond/Al bonding interface with high thermal stability^[6].

In this work, we present the direct bonding of diamond and Cu using SAB at room temperature. The optical microscope image of the diamond/Cu bonded sample surface without annealing is shown in Fig. 1. Although a small unbonded region was observed on the upper left side of the bonded sample, an about 99 % area bonding of diamond and Cu was achieved.

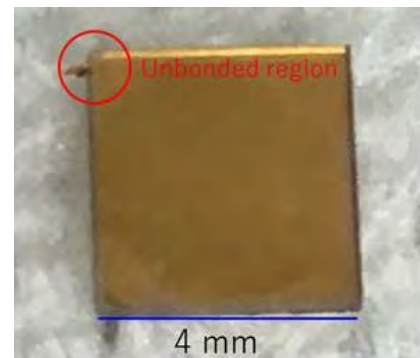


Figure 1. The optical microscope image of the diamond/Cu bonded sample surface without annealing.

References:

- [1] J. Isberg, J. Hammersberg, E. Johansson, T. Wikström, D. J. Twitchen, A. J. Whitehead, S. E. Core, and G. A. Scarsbrook, *Science* 297 (2002) 1670.
- [2] A. T. Collins, In *Properties and Growth of Diamond*, IEE: Inspec, London, 1994.
- [3] M. Kasu, K. Ueda, H. Ye, Y. Yamauchi, S. Sasaki, and T. Makimoto, *Electron. Lett.* 41 (2005) 1249.
- [4] M. Kasu, H. Sato, and K. HIRAMA, *Appl. Phys. Express* 5 (2012) 025701.
- [5] H. Umezawa, Y. Kato, and S. I. Shikata, *Appl. Phys. Express* 6 (2013) 011302.
- [6] J. Liang, Shoji Yamajo, Martin Kuball, N. Shigekawa, *Scripta Materialia* 159 (2019) 58.



Bonding strength evaluation of Al foil/AlN junctions by surface activated bonding

S. Horikawa, S. Morita, J. Liang, Y. Kaneko, and N. Shigekawa
 Graduate School of Engineering, Osaka City University,
 3-3-138 Sugimoto, Sumiyoshi-ku, Osaka 558-8585, Japan
 m18tb050@hg.osaka-cu.ac.jp

Abstract:

The thermal tolerance of widegap semiconductors, which largely outperforms of that of conventionally-used Si, has not yet fully exploited in the present power electronics modules since the highest temperature of normal operations of such modules is limited by several factors such as the thermal tolerance of die attaches and the thermal resistance of ceramic plates^[1]. We previously fabricated Al-foil/AlN and SiC-die/Al-foil/AlN junctions by using the surface-activation bonding (SAB), i.e., without using die attaches, and confirmed that no fractures appeared at the Al/AlN interfaces even after annealing at 600 °C. We also showed that bonded SiC Schottky diodes normally operated in an ambient temperature up to 300 °C^[2].

In this work, we fabricated an Al foil/AlN junction by An Al foil/AlN junction is fabricated by bonding a 30- μm Al foil and a 650- μm AlN plate at room temperature and 473 K. The peel strengths of the two junctions were evaluated by a 180° peel test in a schematic shown in Fig. 1. The relationship between the peel strength and the stroke of the respective junctions is shown in Fig. 2. The peel strength, which revealed ununiform features, was ~ 30 and ~ 60 N/m for the junctions fabricated by the room-temperature bonding and the 473-K bonding, respectively.

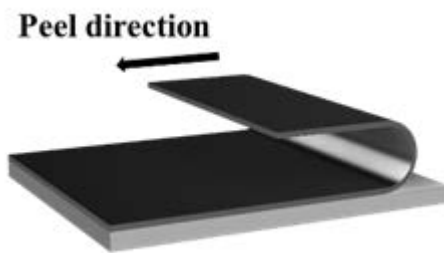


Fig. 1. Schematic of 180° peel test.

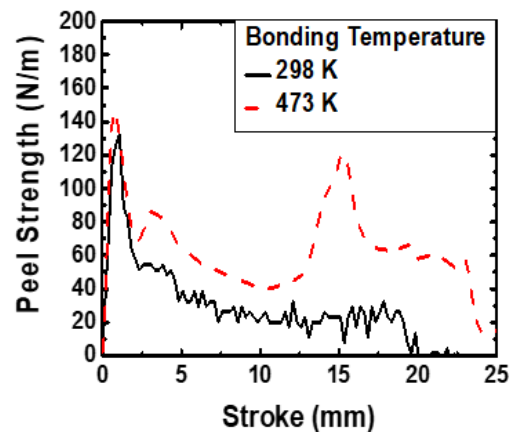
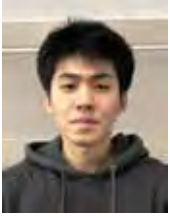


Fig. 2. Peel Strength of Al foil/AlN junctions.

References:

- [1] R. Kisiel, et al. *Microelectronics Reliability*, vol. 49, pp. 627–629, 2009.
- [2] S. Morita, et al. *ECS Trans.*, vol.86, pp. 137-142, 2018.



Analysis of SiC/Si Bonding Interface with Thermal Annealing Treatment by XPS

Zexin Wan, Jianbo Liang, Naoteru Shigekawa

Graduate School of Engineering, Osaka City University, 3-3-138 Sugimoto, Sumiyoshi, Osaka 558-8585, Japan

Abstract: It was reported that the reaction between Schottky contacts and SiC layers limits their thermal tolerance [1]. The usage of heavily doped Si substrates as substitute for Schottky contacts is a practicable method to solve the problem. We applied the surface-activated bonding (SAB) to fabricate the SiC/Si heterojunctions [2]. During the irradiation of fast atom beam (FAB) of Ar, damages were introduced to the substrate and the electrical properties of the SiC/Si junctions were largely affected. We previously found that the effects of damages were recovered by the thermal treatment. In this research, the variation in properties of SiC/Si bonding interfaces due to the thermal treatment is investigated by using X-ray photoelectron spectroscopy (XPS). The process of experiment is shown in Fig.1. We annealed the SiC/Si junctions at 400, 700, and 1000°C, and measured their current-voltage characteristic at room temperature. Then we removed the Si substrate and analyzed the exposed surface of SiC by using XPS. The C1s core level spectra of the respective SiC surfaces are shown in Fig.2. By fitting the XPS spectra, we find that the annealing of junctions brings about the shift in binding energy of C-Si bonding, which is in correlation with the reverse-bias current of SiC/Si heterojunction. The change in the binding energy is assumed to be attributed to the shift of Fermi level at the SiC surface due to the annealing.

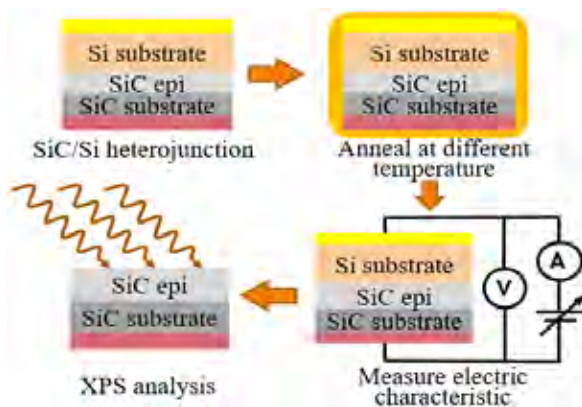


Fig.1 Schematic of the process applied to SiC/Si heterojunction.

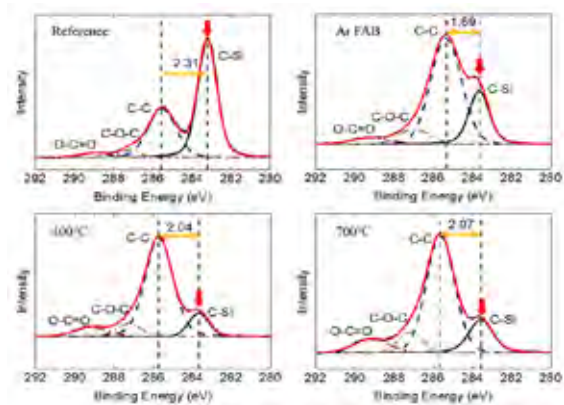


Fig.2. Spectra of C 1s core level of SiC surface

Acknowledge:

The XPS analysis was supported by Prof. Kouichi Tsuji, Graduate School of Engineering, Osaka City University.

References:

- [1] Bhanumurthy K., Schmid-Fetzer R., "Solid-state reaction bonding of silicon carbide (HIP-SiC) below 1000°C" *Materials Science and Engineering A* 220(1):35-40.
- [2] J. Liang, S. Nishida, M. Arai, and N. Shigekawa, "Improved electrical properties of n-n and p-n Si/SiC junctions with thermal annealing treatment." *J. Appl. Phys.* 120, 034504 (2016).

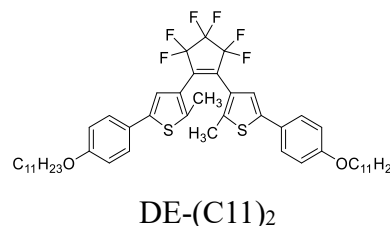


Photoinduced Shape Change of Crystals Composed of a Diarylethene with a Long Alkyl Chain

Takuya Higashiguchi, Daichi Kitagawa, Seiya Kobatake

Department of Applied Chemistry, Graduate School of Engineering,
Osaka City University, Osaka 558-8585, Japan

Diarylethene crystals exhibit various photomechanical behaviors such as contraction, expansion, bending, fragmentation, and twisting, which are expected to be applied to photoactuators [1]. In particular, crystals consisting of a diarylethene with a long alkyl group exhibit unique photomechanical behavior accompanying a reversible thermodynamic single-crystal-to-single-crystal phase transition [2]. In this study, we investigated on crystal shape changes of a diarylethene having undecyl group at both sides (DE-(C11)₂) upon photoirradiation.



Upon irradiation with UV light, the crystal bent toward the incident light, but the degree of bending depended on the illumination directions (i.e. left or right) as shown in Figure 1. Furthermore, when another plane of the rod-like crystal was irradiated with UV light, the crystal twisted toward the incident light. The degree of twisting also depended on illumination directions as shown in Figure 2. Moreover, in the course of study, it was found that crystals of DE-(C11)₂ were "twin crystal", as can be seen from single crystal X-ray diffraction analysis. The crystals always have striations at twin boundaries as observed by scanning electron microscopy. The two crystals in the twin crystal have different thickness.

These photomechanical behaviors will be discussed based on the molecular packing of a diarylethene and each thickness in the twin crystal.



Figure 1. Photoinduced bending behavior depending on illumination sides. UV irradiation was performed for 10 s.



Figure 2. Photoinduced twisting behavior depending on illumination sides. UV irradiation was performed for 10 s.

[1] M. Irie, T. Fukaminato, K. Matsuda, S. Kobatake, *Chem. Rev.*, **2014**, 114, 12174-12277.

[2] D. Kitagawa, K. Kawasaki, R. Tanaka, S. Kobatake, *Chem. Mater.*, **2017**, 29, 7524-7532.



Photoluminescence Switching of Quantum Dot Coated with Diarylethenes by Photochromic Reaction

Yuya Seto, Daichi Kitagawa, DaeGwi Kim, Seiya Kobatake
 Graduate School of Engineering, Osaka City University,
 3-3-138 Sugimoto, Sumiyoshi-ku, Osaka 558-8585, Japan

Diarylethene (DE) is one of the photochromic compounds which has excellent properties such as fast response and high repeating durability^[1]. Quantum dots (QD) have high emission quantum yield and narrow emission band^[2]. Research on photoluminescence on/off switching of QD coated with DE has been conducted so far, but no report shows the high quenching ratio^[3]. In this study, CdSe/ZnS core-shell type of QDs coated with DE (QD-DE) were synthesized (Fig. 1) and the photoluminescence on/off switching behavior accompanying with the photochromic reactions was investigated.

The photoluminescence intensity drastically decreased with increasing absorption intensity of the DE closed-ring form, as shown in Fig. 2. The photocyclization conversion increased with the irradiation time, but the rate of the conversion became slow with increasing coated number of DE, as shown in Fig. 3a. On the other hand, the F/F_0 value relative to the photocyclization conversion largely decreased with increasing coated number of DE as shown in Fig. 3b. We succeeded in fabricating quantum dots coated with diarylethenes exhibiting fast quenching speed and high contrast of photoluminescence on/off switching.

References:

- [1] M. Irie, T. Fukaminato, K. Matsuda, S. Kobatake, *Chem. Rev.* **2014**, 114, 12174-12277.
- [2] W. W. Yu, L. Qu, W. Guo, X. Peng, *Chem. Mater.* **2003**, 15, 2854-2860.
- [3] S. A. Díaz, L. Giordano, T. M. Jovin, E. A. Jares-Erijman, *Nano Lett.* **2012**, 12, 3537-3544.

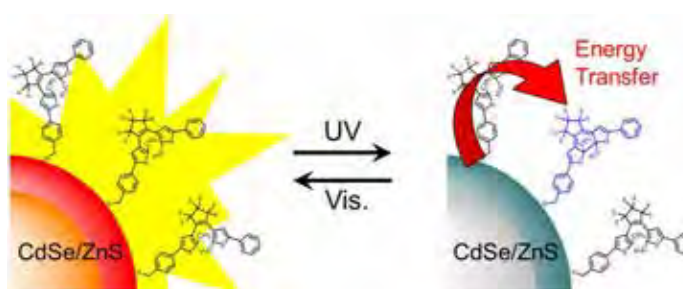


Figure 1. Schematic illustration of photochromism and photoluminescence ON/OFF switching of QD-DE.

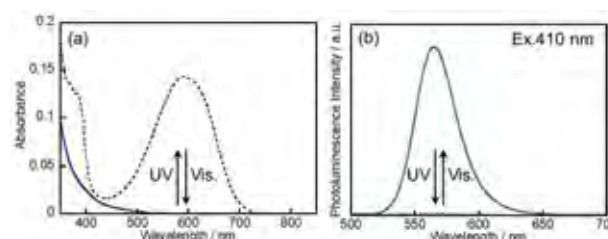


Figure 2. (a) Absorption and (b) photoluminescence spectral changes of QD-DE (DE/QD = 87.4) in toluene upon alternating irradiation with 313 nm light and visible light.

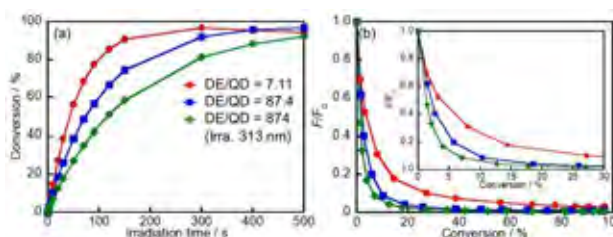


Figure 3. (a) Photocyclization conversion relative to irradiation time and (b) normalized photoluminescence intensity relative to photocyclization conversion of QD-DE.



Bright and Tunable Emission of BODIPY in Solid State

Katsuya Shimizu, Seiya Kobatake

Department of Applied Chemistry, Graduate School of Engineering,
Osaka City University, Osaka 558-8585, Japan

Boron dipyrro methane (BODIPY) shown in **Figure 1** has attracted much attention because of high fluorescence quantum yield (Φ_f) and molar extinction coefficient (ϵ) in solution. However, Φ_f significantly decreases and the emission spectrum is red-shifted due to intermolecular interaction such as π - π stacking and reabsorption of fluorescence derived from high planarity and a small Stokes shift in

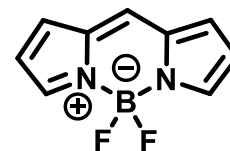


Figure 1. Typical structure of BODIPY.

concentrated solution and in the solid state [1]. If it is easily possible to change the emission color using a single fluorophore without molecular modification and to create solid emissive BODIPY, then that strategy would be very useful for application to optoelectronic materials for solid-state dye lasers and organic light-emitting diodes. Here, we report on the design and fabrication of random copolymers (poly(BO_x-co-St_y)) consisting of BODIPY monomer (BO) and styrene (St) to achieve multi-color and efficient emission in the solid state using St as a spacer (**Figure 2**). As shown in **Figure 3**, the emission color of the resulting copolymers changed from green to red by changing the content of BO from 0.042 to 100 mol%. Φ_f also increased with the content of St ($\Phi_f = 0.05$ -0.88) because the intermolecular distance between the BO fluorophores became longer. In particular, poly(BO_x-co-St_y) ($y/x = 2400$) exhibited a very high Φ_f (0.88) which is the highest value among BODIPY derivatives in the solid state reported to date [2].

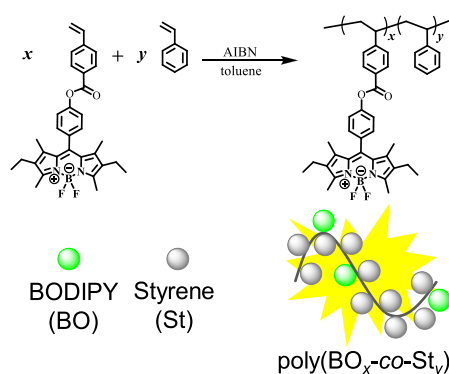


Figure 2. Synthetic scheme of poly(BO_x-co-St_y).

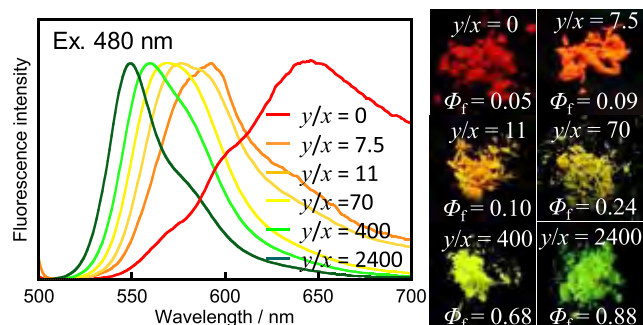


Figure 3. Fluorescence spectra of poly(BO_x-co-St_y) in the bulk powder excited with 480 nm light.

References:

- [1] A. Loudet, K. Burgess, *Chem. Rev.*, **2007**, 107, 4891-4932.
- [2] K. Shimizu, D. Kitagawa, S. Kobatake, *Dyes Pigm.*, **2019**, 161, 341-346.



Simultaneous observation of nanoparticles and hexane droplets in hexane/water emulsion by quick freeze replica electron microscopy

Kazuya Tamejima¹, Takuya Okamoto¹, Yuhei O Tahara^{1,2},
Makoto Miyata^{1,2}, Tomoyuki Yatsunami^{1,2}

¹Graduate School of Science, Osaka City University, Japan

²The OCU Advanced Research Institute for Natural Science and Technology,
Osaka City University, Japan

Gold nanoparticles (AuNPs) are widely used as catalysts and biomedical materials. Femtosecond laser irradiation to gold (III) chloride trihydrate (HAuCl₄) aqueous solution has been reported as one of the single-nano-sized AuNPs synthesis methods [1]. However, a dispersant, which is indispensable to control particle size, might contaminate the resultant AuNPs. We recently succeed synthesizing single-nano-sized AuNPs in hexane/water mixture by femtosecond laser irradiation. The key to form single-nano-sized AuNPs without the use of dispersant is the emulsion formed by stirring HAuCl₄ aqueous solution and hexane. In this study, we try to observe both AuNPs and hexane droplets in water by quick freeze replica electron microscopy to clarify the AuNPs production mechanism.

Hexane / HAuCl₄ aqueous solution was exposed to femtosecond laser pulses (0.8 μm, 40 fs, 0.4 mJ, 1 kHz). The AuNPs collected from water layer was observed by a transmission electron microscope (TEM). The mean diameter of AuNPs was 6.1±2.0 nm (Fig. 1a, *n* = 300). It is emphasized that the probability of capturing droplets is extremely small since the quick freeze replica method samples only a small part of solution. Therefore, we optimized pre-freezing operation procedures, freezing tools, fracturing position, and sample sublimation time. As a result, the shape of hexane droplet and AuNPs was successfully transferred to the replica made of platinum (Fig.1b, thickness 1.3 nm). The mean diameter of AuNPs on the hexane droplet was 12 nm (*n* = 65). We are now planning to improve the experimental conditions for better statistics.

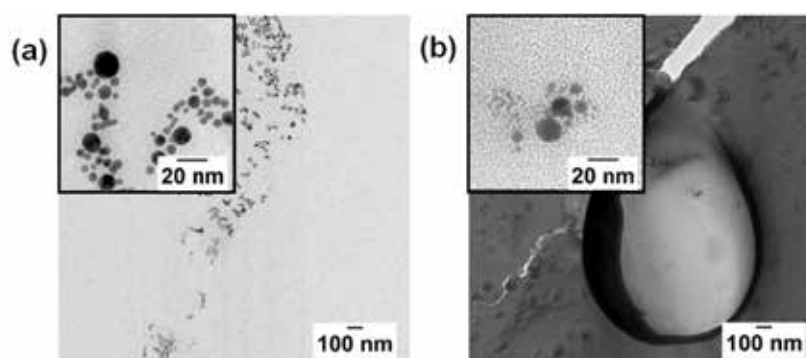


Fig. 1 TEM images of (a) solution and (b) replica.

The mean diameter of AuNPs on the hexane droplet was 12 nm (*n* = 65). We are now planning to improve the experimental conditions for better statistics.

[1] Nakamura, T.; Mochidzuki, Y.; Sato, S., *J. Mater. Res.*, **2008**, 23(4), 968–974.



Study on Micro-Tomographically Functional Imaging of Blood Flow in Vascular Plexuses using Optical Coherence Doppler Velocigraphy

Daisuke FURUKAWA¹, Souichi SAEKI¹,
, Takafumi ITO², Yoshiaki NISHINO², Yusuke HARA^{1,3}

¹ Graduate School of Engineering, Mechanical & Physical Engineering, Osaka City
University. 3-3-138, Sugimoto, Sumiyoshi-ku, Osaka, 558-8585

² TOKOTAKAOKA Co., Ltd, Hamamatsu, Japan

³ SHISEIDO Research Center, Yokohama, Japan

Abstract:

The skin aging process, e.g. wrinkles and saggings, caused by not only aging but also ultraviolet irradiation, could be related to the depression of metabolic function. The microcirculation system should be an important guideline of skin care for the anti/smart-aging. Rheological behavior of interstitial in epidermal and dermal tissue, including blood micro-circulation, can vary skin mechanics in micro scale, i.e. visco-elasticity. Therefore, an *in vivo* quantitative measurement of capillary blood flow velocity is crucial to clarify their properties. The purpose of this study is to visualize the tomographic flow velocity of red blood cell in capillaries below human epidermal skin using Optical Coherence Doppler Velocigraphy, i.e. OCDV [1]. This is constructed on a low coherence interferometer [2], which is based on Hilbert transform and adjacent auto-correlation. In order to validate OCDV system, this was *in vivo* applied to human forearm skin under the condition with or without vasodilation, respectively. As a result of skin tomography obtained by OCDV, A *en-face* cross-sectional MIP can display horizontal networks of capillary blood vessels. Additionally, it was confirmed that capillary vasculature and blood velocity can be visualized tomographically even in the upper subpapillary layer. In summary, OCDV system could be quite useful for a micro-tomographic imaging of blood flow velocity of capillary vessels inside skin.

References:

- [1] Daisuke Furukawa, et al., “In vivo Micro-Tomographic Visualization of Capillary Angio-Dynamics Around Upper Dermis Under Mechanical Stimulus Using Low Coherence Interferometer “Optical Coherence Doppler Velocigraphy”, American Journal of Physics and Application, Vol.6(4), (2018), pp.89-96.
- [2] Joseph M. Schmitt, “Optical Coherence Tomography (OCT): A Review”, IEEE Journal on Selected Topics in Quantum Electronics, Vol.5, No.4 (1999), pp.1134-1142.

Development of Micro-tomographic Visualizing System of Mechanical Properties inside Regenerated Tissue using UA-OCDV

Koji YAMANE ¹, Daisuke FURUKAWA ², Souichi SAEKI ²

¹ Department of Mechanical Engineering, Faculty of Engineering, Osaka City University.

3-3-138, Sugimoto, Sumiyoshi-ku, Osaka, 558-8585

² Graduate School of Engineering, Mechanical & Physical Engineering, Osaka City University. 3-3-138, Sugimoto, Sumiyoshi-ku, Osaka, 558-8585

Abstract:

In recent years, the regenerative therapy of osteoarthritic cartilage has attracted attention due to clinical transplantation of autologous cultured cartilage. However, a non-contact and invasive diagnosing method of bio-mechanical functions, e.g. viscosity and elasticity, has never been established yet. The purpose of this research is to construct and validate the ultrasonic-assisted Doppler OCT system (UA-OCDV), which can provide viscoelastic characteristics inside tissue tomographically and non-contactly using a high intensity focused ultrasound transducer as a loading device. UA-OCDV was applied to porcine cartilages with or without collagenase treatment. Figure 1 shows tissue discrimination via tomographic phase map, where left and right sides are normal and digested cartilage, respectively. Consequently, UA-OCDV can visualize water permeability inside tissue micro-tomographically. Furthermore, this is effective to a non-contact diagnosing tool of viscoelastic properties correlated with water permeability.

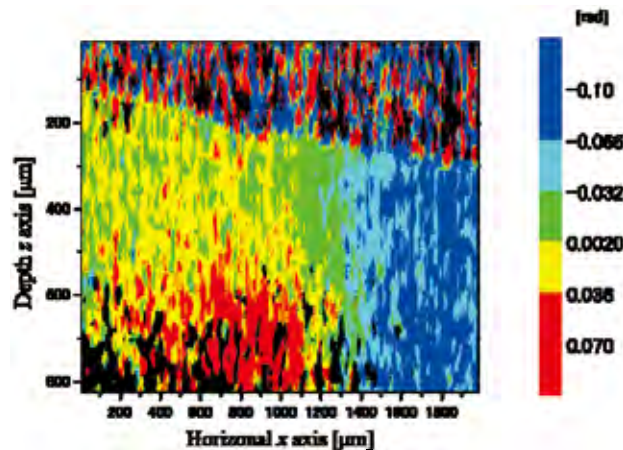


Fig.1 Cross-section color map of phase difference to acoustic radiation pressure

Construction on Medical Diagnosing System by Photo-thermal Doppler OCT (PT-OCDV) using photosensitizer

Miki YANAGISA¹, Daisuke FURUKAWA², Souichi SAEKI²

¹. *Department of Engineering, Mechanical Engineering, Osaka City University. 3-3-138,*

Sugimoto, Sumiyoshi-ku, Osaka, 558-8585

². *Graduate School of Engineering, Mechanical & Physical Engineering, Osaka City University. 3-3-138, Sugimoto, Sumiyoshi-ku, Osaka, 558-8585*

Abstract:

Medical diagnosis using near-infrared fluorescence emitted from a photosensitizer [1], e.g. Indocyanine green (ICG), has attracted attention as a clinical and surgical visualizing tool of tumor and vasculature. The purpose of this study is to construct and validate an *in vivo* micro-tomographic visualizing system of pharmacokinetics of delivered drug, namely PT-OCDV. The proposed system, based on Doppler OCT, can provide tomographic detection of photo-thermal effect by a photosensitizer inside tissue. *in vivo* animal experiment was carried out using a mouse administered intraperitoneally with ICG. As a result, PT-OCDV displayed the tomographic distribution of not only capillary blood flow but also drug diffusion to tissue. It was proven that the present system had good potential as a diagnostic modality of various disease and Drug Delivery System.

References:

[1] Nakamichi, Y., et al , Journal of Biomechanical Science and Engineering, Vol.12, No.2, 2017, 16-00591.